Distance and Reddening of the Isolated Dwarf Irregular Galaxy NGC 1156

Sang Chul KIM[1], Hong Soo PARK[2], Jaemann KYEONG[1], Joon Hyeop LEE[1], Chang Hee REE[1], and Minjin KIM[1,3,4]

[1]*Korea Astronomy & Space Science Institute, Daejeon 305-348, Korea*

[2] *Department of Physics and Astronomy, Seoul National University, Seoul 151-742, Korea*

[3] *The Observatories of the Carnegie Institution for Science, 813 Santa Barbara Street, Pasadena, CA 91101, USA*

[4] *KASI-Carnegie Fellow*

sckim@kasi.re.kr, hspark@astro.snu.ac.kr, jman@kasi.re.kr, jhl@kasi.re.kr, chr@kasi.re.kr, mkim@kasi.re.kr

To appear in PASJ 2012 April 25, Vol. 64, Issue 2

ABSTRACT

We present a photometric estimation of the distance and reddening values to the dwarf irregular galaxy NGC 1156, which is one of the best targets to study the isolated dwarf galaxies in the nearby universe. We have used the imaging data sets of the *Hubble Space Telescope (HST)* Advanced Camera for Surveys (ACS) High Resolution Channel (HRC) of the central region of NGC 1156 ($26'' \times 29''$) available in the *HST* archive for this study. From the $(U-B, B-V)$ color-color diagram, we first estimate the total (foreground + internal) reddening toward NGC 1156 of $E(B-V) = 0.35 \pm 0.05$ mag, whereas only the foreground reddening was previously known to be $E(B-V) = 0.16$ mag (Burstein & Heiles) or 0.24 mag (Schlegel, Finkbeiner, & Davis). Based on the brightest stars method, selecting the three brightest blue supergiant (BSG) stars with mean B magnitude of $\langle B(3B) \rangle = 21.94$ mag and the three brightest red supergiant (RSG) stars with mean V magnitude of $\langle V(3R) \rangle = 22.76$ mag, we derive the distance modulus to NGC 1156 to be $(m-M)_{0,BSG} = 29.55$ mag and $(m-M)_{0,RSG} = 29.16$ mag. By using weights of 1 and 1.5 for the distance moduli from using the BSGs and the RSGs, respectively, we finally obtain the weighted mean distance modulus to NGC 1156 $(m-M)_0 = 29.39 \pm 0.20$ mag ($d = 7.6 \pm 0.7$ Mpc), which is in very good agreement with the previous estimates. Combining the photometry data of this study with those of Karachentsev et al. gives smaller distance to NGC 1156, which is discussed together with the limits of the data.

Subject headings: galaxies: dwarf irregular galaxies — galaxies: photometry — galaxies: individual: NGC 1156 — globular clusters: individual: NGC 104 (47 Tucanae)

1. INTRODUCTION

Dwarf galaxies are an important class of galaxies in studying the evolution of galaxies as well as the cosmological evolution of the universe. They have much simpler structures than larger/giant galaxies, and are prone to be affected by small perturbations. It is also easy to observe and study the whole systems of dwarf galaxies because of their small sizes (Kim & Lee 1998; Kyeong et al. 2006; Cole et al. 2007; Kyeong et al. 2010). Isolated dwarf galaxies are even better targets for studying the evolution of the system since they are not affected by any environmental effects so that any kind of causes and effects reside in the system itself.

NGC 1156 (UGC 2455, Vorontsov-Velyaminov [VV] 531, PGC 11329, KIG 0121, IRAS F02567+2502)

is an isolated, Magellanic type dwarf irregular (dIrr) galaxy with the morphological type of IB(s)m V-VI (Sandage & Binggeli 1994; de Vaucouleurs et al. 1991). This galaxy has boxy-like shape and bright blue patches implying an active star formation stage, though not triggered by any external tidal perturbations (Karachentsev et al. 1996). NGC 1156 is one of the highly isolated and less disturbed galaxies, and its nearest neighbors are UGC 2684 and UGC 2716, located more than 10° away from NGC 1156 (Karachentsev et al. 1996; Minchin et al. 2010). Studying the star formation rate, mass loss rate, current star formation activity, etc. for NGC 1156 is very interesting, because this galaxy is not thought to be disturbed/triggered by any nearby objects (Hunter & Elmegreen 2004). Recently, using the 21 cm line of neutral hydrogen (H I) observed with the Arecibo *L*-band Feed Array, Minchin et al. (2010) found a new small dwarf galaxy dubbed AGES J030039+254656 at 35′ north-northeast of NGC 1156 (80 kpc in projection, $\alpha_{J2000.0} = 03^{\rm h}00^{\rm m}38.6^{\rm s}$, $\delta_{J2000.0} = +25°47'02''$). This galaxy has an H I flux of 0.114 ± 0.032 Jy km s^{-1}, giving it a neutral hydrogen mass of $(1.63 \pm 0.46) \times 10^6$ $M_\odot$. Minchin et al. (2010) estimated that the star formation rate and H I mass of this galaxy are both around three orders of magnitude lower than in the case of NGC 1156 and concluded that it is unlikely that AGES J030039+254656, in its current position, could be exerting any significant tidal force on NGC 1156.

Although there have been many studies on NGC 1156 (especially the H II regions and CO content; see table 1 below), the distance estimate to this galaxy is only based on two studies Karachentsev et al. (1996) and Tully (1988). Karachentsev et al. (1996) estimated the distance to NGC 1156 to be $d = 7.8 \pm 0.5$ Mpc ($(m-M)_0 = 29.46 \pm 0.15$ mag) using the brightest stars method with V (300 s exposure time) and I (300 s) CCD images for the central $80'' \times 120''$ area obtained at the Special Astrophysical Observatory (SAO) 6 m telescope. From the Tully-Fisher relation, Tully (1988) obtained the distance to NGC 1156 of 6.4 Mpc ($(m-M)_0 = 29.02 \pm 0.40$ mag). There is no estimate for the total (foreground + internal) reddening toward NGC 1156, and there are only two foreground reddening estimates to NGC 1156: $E(B-V) = 0.16$ mag and 0.24 mag measured by Burstein & Heiles (1984) and Schlegel et al. (1989), respectively.

Thanks to the unprecedented resolving power of the *Hubble Space Telescope (HST)*, we are able to resolve individual stars at the center of galaxy NGC 1156. This allows us to investigate the color-color diagram of the central stars of NGC 1156 and hence make an accurate estimation of the reddening and then the distance modulus to this galaxy. In this paper, we present a new estimate of the distance and (total) reddening to NGC 1156 using the photometry from the *HST* archive imaging data. This paper is arranged as follows. In section 2, we describe the data set used in this study, and we present data reduction and transformation into the standard $UBVI$ photometric system in section 3. In section 4, we show the color-magnitude diagrams, and derive the reddening and distance to NGC 1156. We discuss the results in section 5, and finally summarize the results in section 6.

2. DATA

For this study, we used the imaging data sets of *HST* Advanced Camera for Surveys (ACS) High Resolution Channel (HRC) on NGC 1156 available in the *HST* archive. While Wide Field Channel (WFC) is the widely used camera of the ACS, HRC is one of the three electronic cameras of ACS together with Solar Blind Channel (SBC), and is designed for high angular resolution imaging and coronagraphy for the wavelength range of 2,000 – 11,000Å. The field-of-view of HRC is $26'' \times 29''$ (1024×1024 SITe CCD), with pixel size of $0.025'' \times 0.028''$ (21μm/pixel).

The data used in this study were obtained on 2005 September $5-6$ (UT) with F330W, F435W, F550M, F814W, and F658N filters through *HST* observing program 10609 (P.I.: William Vacca). The accumulated exposure times were 1780 s (4×445 s) for the F330W band, 592 s (4×148 s) for the F435W band, 780 s (4×195 s) for the F550M band, 364 s (4×91 s) for the F814W band, and 240 s for the F658N band, and for this study we used the images obtained in the F330W, F435W, F550M, and F814W bands. Figure 1 displays the grey-scale image of NGC 1156 ($5' \times 5'$) taken from the Digitized Sky Survey (DSS), and figure 2 shows the *HST* ACS/HRC F814W image of NGC 1156 ($26'' \times 29''$) which is the very central region (inner

box) of NGC 1156 in figure 1.

3. DATA REDUCTION

3.1. Photometry

Photometry of NGC 1156 was carried out for the data taken by *HST* ACS/HRC using the DOLPHOT package developed by Dolphin (2000a,b). The DOLPHOT routine performs point spread function fitting to the stars and gives the magnitudes in the standard Johnson system as well as instrumental magnitudes in the *HST* filter system. DOLPHOT uses zeropoints and transformation coefficients of Sirianni et al. (2005), which was recently revised (see *HST* ACS Web page, http://www.stsci.edu/hst/acs/analysis/zeropoints/).

Figure 3 shows the photometric errors from the DOLPHOT package as a function of magnitude. The DOLPHOT gives five classifications for objects (object 1 : good star; object 2 : possible unresolved binary, two stars combined during photometry iterations; object 3 : bad star, centered on saturated pixel or bad column; object 4 : single-pixel cosmic ray or hot pixel; object 5 : extended object), and here we plot only objects with reliable measurement (i.e., flagged as object type 1; $N = 5580$).

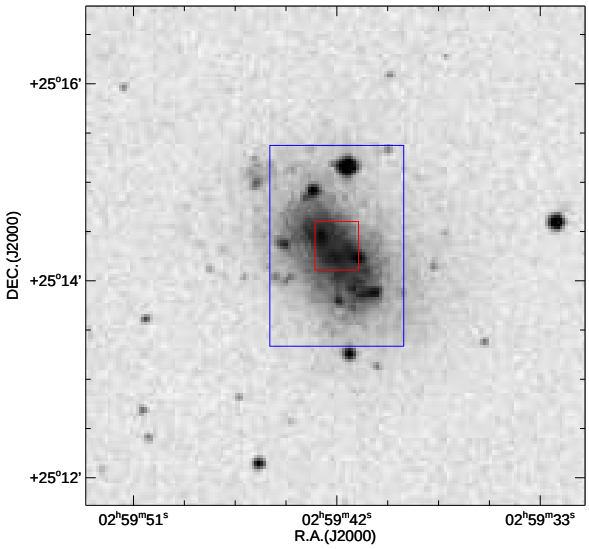

Fig. 1.— Gray-scale second generation Digitized Sky Survey (DSS) image of NGC 1156. The size of the field of view is $5' \times 5'$. North is at the top and east is to the left. The coordinate of NGC 1156 given by the NASA/IPAC Extragalactic Database (NED) is $(\alpha_{J2000}, \delta_{J2000}) = (02^h\ 59^m\ 42.19^s, +25^\circ\ 14'\ 14.2'')$, which is also the field center in this image. The inner box denotes the area $(26'' \times 29'')$ covered by the *HST* images in this study (also shown in figure 2), and the outer box shows the area $(80'' \times 120'')$ covered by Karachentsev et al. (1996).

3.2. Transformation to the $UBVI$ system

We use the $UBVI$ filter system for the analysis of the photometric properties and determination of the distance to NGC 1156. Although the DOLPHOT package effectively converts the ACS filter system into the $UBVI$ system using the coefficients of Sirianni et al. (2005), the transformation from F550M to V-band is not provided. While the recent transformation relations from the *HST* ACS/WFC system (including F550M filter) to the $BVRI$ photometry were given by Saha et al. (2011), their relations are solely based on the WFC, excluding the HRC. We, therefore, transform the F550M magnitude into the V magnitude as described below, while the conversions from the F330W, F435W, and F814W filters to the U, B, and I bands, respectively, are made by the DOLPHOT package.

First, we transform the F550M magnitudes into

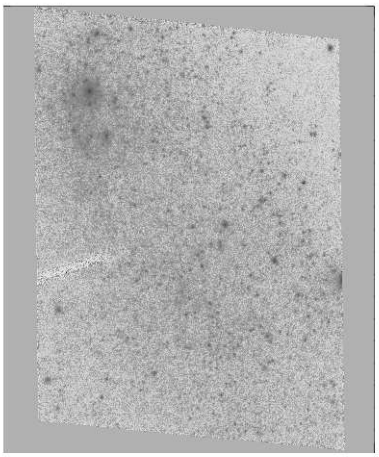

Fig. 2.— Geometric distortion corrected *HST* ACS/HRC F814W image of NGC 1156. The field of view is about $26'' \times 29''$, which shows the very central region of NGC 1156 shown in figure 1. North is at the top and east is to the left. The coordinate of the center is (α_{J2000}, δ_{J2000}) = (02^h 59^m 42.2^s, $+25^\circ$ $14'$ $20.2''$). The bar feature on the (lower) left is the "coronagraphic finger" of the ACS/HRC.

the F555W magnitudes using the equation

$$\begin{aligned} F555W &= F550M + 0.232(F550M - F814W) \\ &\quad \text{for } (F550M - F814W) < 1.337 \text{ mag} \\ F555W &= F550M + 0.311 \\ &\quad \text{for } (F550M - F814W) \geq 1.337 \text{ mag} \end{aligned} \quad (1)$$

to use the transformation coefficients from F555W to V given by Sirianni et al. (2005) in the DOLPHOT package.

Equation (1) is derived using the photometry of the stars in the globular cluster 47 Tucanae (NGC 104) obtained from the *HST* ACS/HRC images and using the Padova isochrones (Marigo et al. 2008). Figure 4 (a) shows the color-color diagram of the stars in the globular cluster 47 Tuc obtained from the *HST* ACS/HRC images with F550M, F555W and F814W filters. Small dots show the stars of 47 Tuc from the DOLPHOT package with object type 1 and F550M error $<$ 0.05 mag. Among these stars we selected stars with F550M error $<$ 0.006 mag and performed the ordinary least-squares fitting (Isobe et al. 1990) with 3-sigma clipping for these stars, which are shown in circles and a blue slanted line denoting the upper part of the equation (1). Since there are not enough number of stars to use at the red part (F550M$-$F814W $\geq$ 1.337 mag), we have used the Padova isochrones (Marigo et al. 2008) as in figure 4 (b). Saviane et al. (2008) find 12+ log (O/H) = 8.23 for NGC 1156 and using the equations [Fe/H] = log (O/H) +3.34 = $-$0.43 dex (Bono et a. 2010) and log Z = 0.977 [Fe/H] $-$1.699 (Bertelli et al. 1994) we assume Z = 0.008 for NGC 1156. The various ages (1, 2, 5, and 12 Gyr) used in figure 4 (b) give little differences and we have used a constant value of 0.311 (lower part of the equation (1)) for the red part of (F550M$-$F814W) $\geq$ 1.337 mag. Figure 4 (c) is the composite of the panels (a) and (b), showing the stars in the globular cluster 47 Tuc (dots for the stars with F550M error $<$ 0.05 mag and small circles for those with F550M error $<$ 0.006 mag), the Padova isochrones with Z = 0.008 and ages of 1 Gyr (triangles) and 12 Gyr (large circles), and the equation (1) plotted in solid line.

To test the efficiency of this method, we compare the V magnitudes transformed from F550M and from F555W for the stars in the globular cluster 47 Tuc in figure 4 (d), where circles are for the stars with F550M error $<$ 0.006 mag shown also as

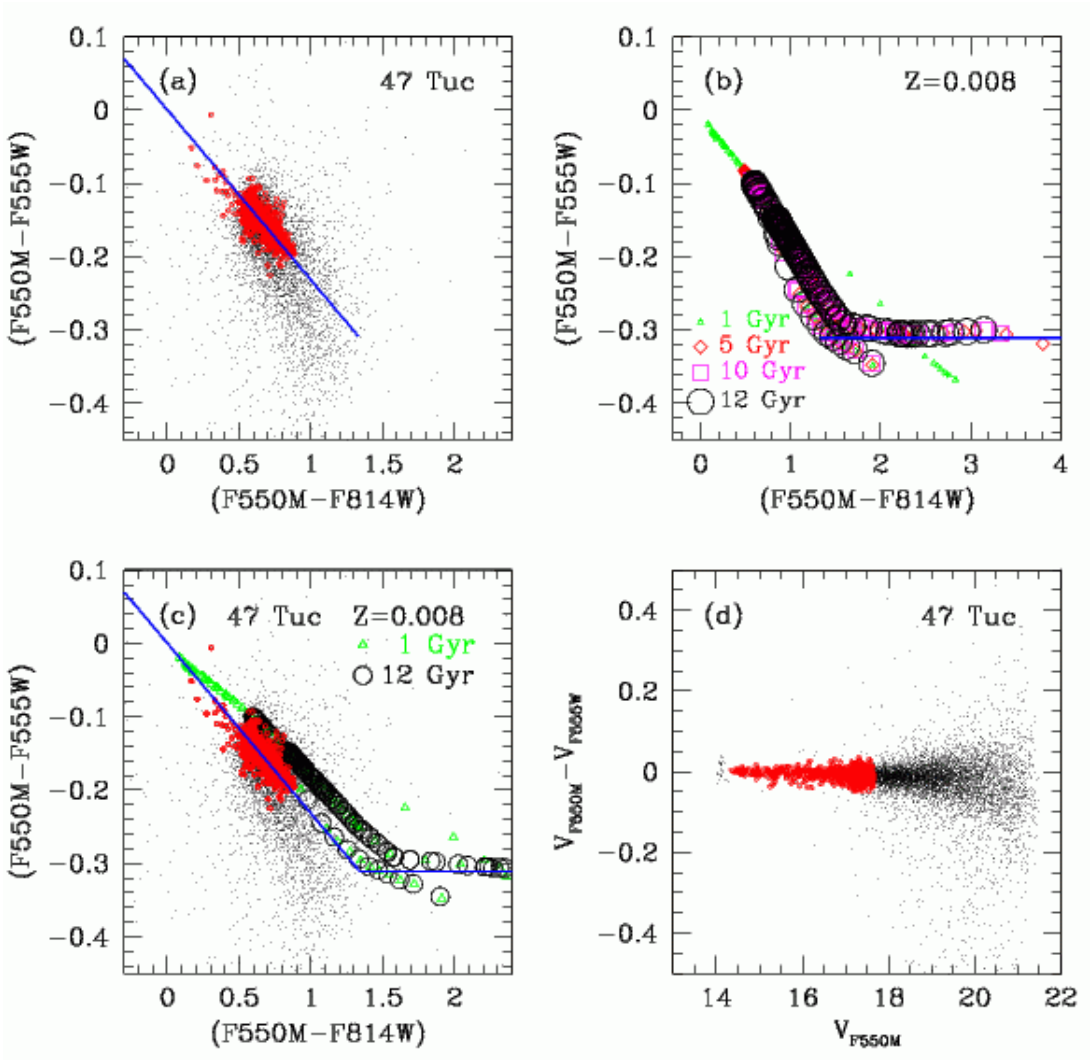

Fig. 4.— (a) The color-color diagram of the stars in the globular cluster 47 Tuc (NGC 104) obtained from the *HST* ACS/HRC images. Small dots are for the stars with F550M error < 0.05 mag. Stars with F550M error < 0.006 mag are selected and used for the ordinary least-squares fitting (Isobe et al. 1990) with 3-sigma clipping, which are shown in circles and slanted line for the blue part of (F550M−F814W) $\lesssim 1.3$. (b) The Padova isochrones (Marigo et al. 2008) with Z= 0.008 and various ages (1, 5, 10, and 12 Gyr) are shown. The constant value determined at (F550M−F814W) $\gtrsim 1.3$ is shown as a horizontal line. (c) Composite of panels (a) and (b), showing the stars of the globular cluster 47 Tuc (dots for the stars with F550M error < 0.05 mag and small circles for the stars with F550M error < 0.006 mag) and the Padova isochrones with Z= 0.008 and ages of 1 Gyr (triangles) and 12 Gyr (large circles). The solid line shows the selected transformation with slope of 0.232 (for the blue part of F550M−F814W ≤ 1.337 mag) and 0 (for the red part of F550M−F814W ≥ 1.337 mag). (d) The difference between the two V magnitudes transformed from F550M and from F555W, which shows very good agreement especially for the stars with small errors (F550M error < 0.006 mag) shown in circles.

circles in panel (a). The two V magnitudes transformed from F550M and from F555W are in very good agreement with each other as seen in figure 4 (d).

4. RESULTS

4.1. Color-Magnitude Diagrams

Figure 5 displays the color-magnitude diagrams (CMDs) for the measured stars (N= 5248) located in the central region of NGC 1156, only with DOLPHOT object type of 1. While blue supergiant (BSG)/blue main sequence stars are clearly seen in the $(V, U-B)$ (figure 5(a)) and $(V, B-V)$ (figure 5(b)) CMDs reaching $B = 21.6$ mag and $V = 21.3$ mag, the $((V, V-I)$ (figure 5(c)) and $(I, V-I)$ (figure 5(d)) CMDs show both the BSG and red supergiant (RSG) stars well, the color of the latter being $(V-I) \sim 2$ mag and reaching up to $V = 22.7$ mag and $I = 20.6$ mag. Red giant branch (RGB) stars are located below the tip of the RGB (TRGB), which might be much fainter than $I \sim 24$ (see figure 5(d)). There should be many asymptotic giant branch (AGB) stars between the RSG and RGB stars (see, e.g., Cioni & Habing (2005)).

If we assume (i) the distance to NGC 1156 to be $d = 7.1 \pm 1.0$ Mpc ($(m-M)_0 = 29.24 \pm 0.31$ mag) given by the NASA/IPAC Extragalactic Database (NED) which is the mean of the two values from Tully (1988) ($(m-M)_0 = 29.02 \pm 0.40$ mag) and Karachentsev et al. (1996) ($(m-M)_0 = 29.46 \pm 0.15$ mag), (ii) the total reddening toward NGC 1156 to be $E(B-V) = 0.35 \pm 0.05$ mag as obtained in the following subsection, and (iii) the I-band absolute magnitude of the TRGB to be $M_{I,TRGB} \approx -4.0 \pm 0.1$ mag (Lee et al. 1993), then the I-band magnitude of the TRGB might be located at $I \sim 25.8$ mag. The U-magnitude calibration from Sirianni et al. (2005) is bifid above and below $(U-B) = 0.2$ mag (see their table 23). At the very color of $(U-B) = 0.2$ mag, the derived U-magnitudes are different by 0.1 mag (see also their figure 22), and this appears to be the reason for the vertical gap-like feature at $(U-B) = 0.2$ mag in the $(V, U-B)$ CMD (figure 5(a)). The cross identification results of the bright stars and star clusters in the *HST* images and the Canada-France-Hawaii Telescope near-infrared images will be shown in a subsequent paper (J. Kyeong et al. in preparation).

4.2. Interstellar Reddening toward NGC 1156

Since NGC 1156 is a dIrr galaxy containing many star forming regions (Barazza et al. 2001), the internal reddening in NGC 1156 might not be negligible and the estimate of the total[1] reddening toward NGC 1156 is important for the photometric studies of this galaxy. However, there are only two foreground reddening values toward NGC 1156. Burstein & Heiles (1984) measured $A_B = 0.66$ mag using 21 cm H I column density and faint galaxy counts method. On the other hand, Schlegel et al. (1989) determined $A_B = 0.968$ mag based on the *COBE*/DIRBE measurement of diffuse infrared emission. By adopting $R_V = 3.1$ and the interstellar extinction law of Cardelli et al. (1989), these values convert to $E(B-V) = 0.16$ mag and 0.24 mag, respectively.

Using the color-color diagram produces a robust method for determining the interstellar reddening value only if UBV photometric data are available. Fortunately, our four filter photometry allows us to derive the interstellar reddening value using the $(U-B, B-V)$ color-color diagram, which is shown in figure 6. The total reddening value, that is foreground reddening plus internal reddening inside the galaxy, is derived shifting the zero age main sequence (ZAMS) relation given by the Padova isochrone ($\log t = 6.0$, Z= 0.008; Marigo et al. (2008), Bertelli et al. (1994), Saviane et al. (2008)) along the reddening line of $E(U-B) = 0.72E(B-V)$ (Gunn & Stryker 1983). Only the stars with U photometric errors smaller than 0.05 mag and object type 1 are included for the fit, which are mostly in the blue main sequence region in the CMD as shown in the panels (a) and (b) of figure 5 as large (red) circles. The photometric errors for these stars in B and V bands are less than 0.06 mag and 0.09 mag, respectively.

The best fit in figure 6 yields $E(B-V) = 0.35 \pm 0.05$ mag for the total reddening value of NGC 1156, which will be used in the derivation of the distance in the next subsection. Since there are several very young star clusters ($\log t < 6.6$)

[1] 'foreground' (found in the Milky Way) + 'internal' (found in the program galaxy)

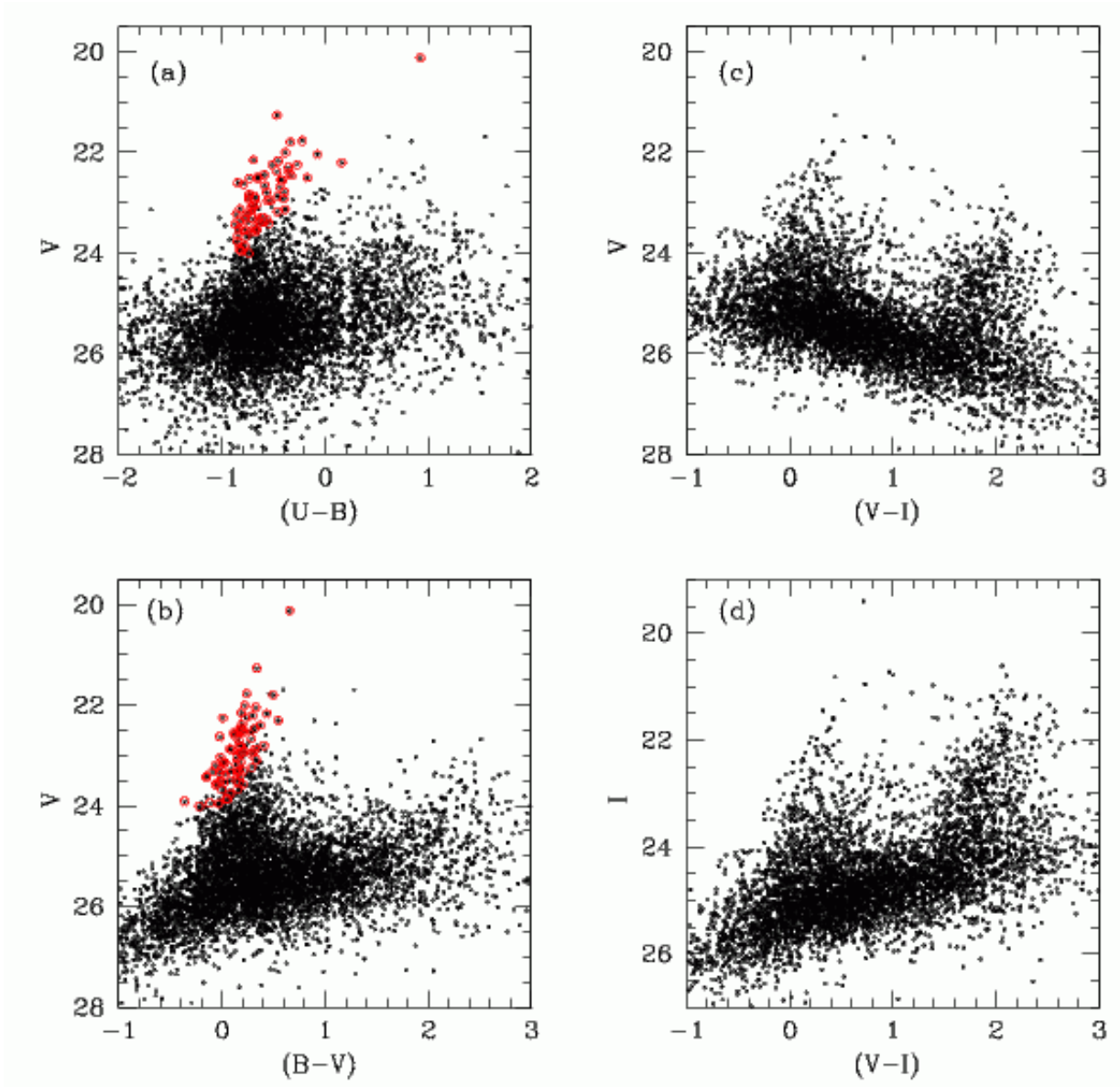

Fig. 5.— Color-magnitude diagrams (CMDs) of NGC 1156 obtained from the *HST* ACS/HRC images. Only the objects of type 1 (good star) are plotted from the DOLPHOT photometry. The large circles in panels (a) and (b) are the objects with U photometric errors smaller than 0.05 mag which are used to estimate the total reddening value toward NGC 1156 in figure 6 below.

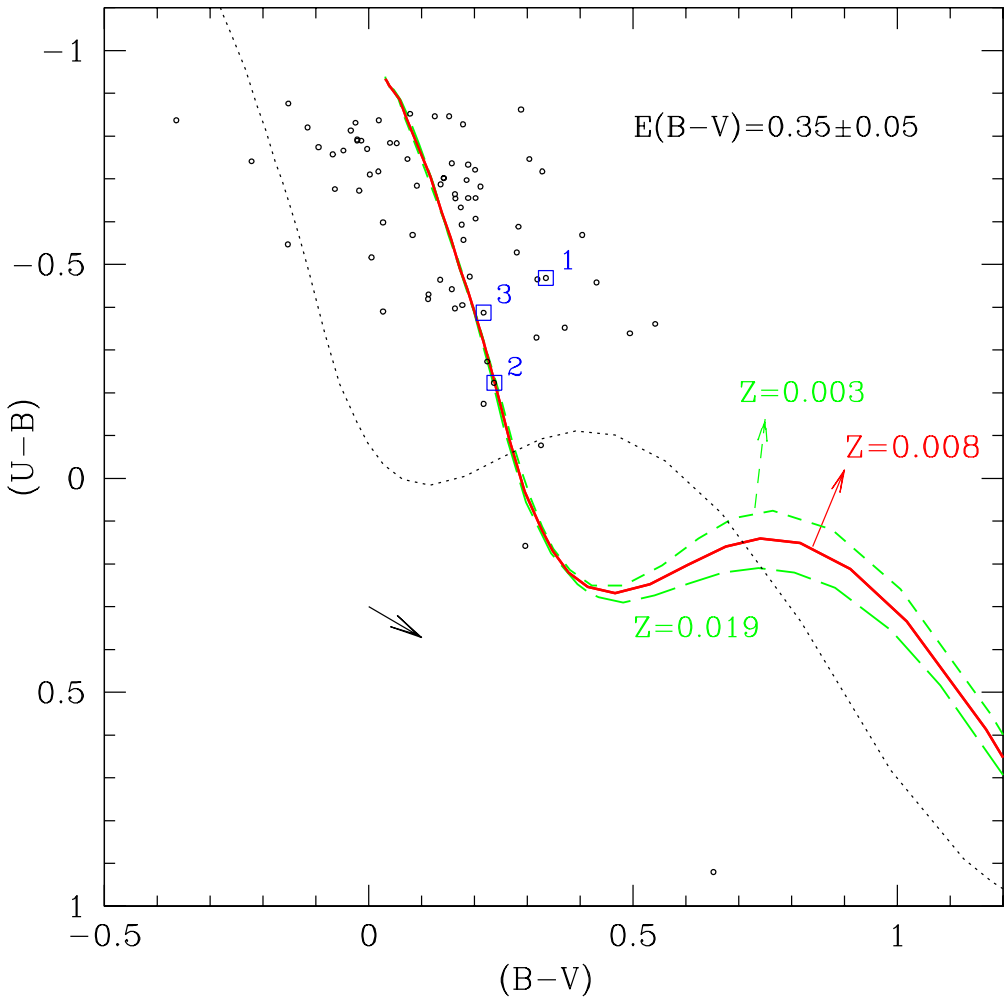

Fig. 6.— $(U-B, B-V)$ color-color diagram of the stars in NGC 1156. The objects with U photometric errors smaller than 0.05 mag and object type 1 are plotted as open circles. The thin dotted line represents the unreddened ZAMS line given by the Padova isochrone (Marigo et al. 2008) with log t = 6.0, Z= 0.008 (Saviane et al. 2008), and the thick solid line represents the ZAMS line reddened by the amount of $E(B-V) = 0.35 \pm 0.05$ mag. The ZAMS lines for Z= 0.003 and Z= 0.019 (both for log t = 6.0) reddened by $E(B-V) = 0.35$ mag are also shown in thick short-dashed and long-dashed lines, respectively, for comparison, where the chosen metallicity gives little difference in obtaining the reddening value. The arrow at $(B-V) \sim 0$ mag is the reddening vector with $E(B-V) = 0.10$ mag. The three, numbered stars with boxes are the BSGs selected in section 4.3 and shown in table 2 in the order named.

in the core region of NGC 1156, the internal reddening that contributed to this value might be due to the gas and dust associated with the star forming regions. The extinction values are calculated for a total-to-selective extinction ratio of $A_V/E(B-V) = 3.1$ using the equations given by Cardelli et al. (1989): $A_B = 4.14E(B-V) = 1.45$ mag, $A_V = 3.1E(B-V) = 1.09$ mag, and $A_I = 1.48E(B-V) = 0.52$ mag.

4.3. Distance to NGC 1156

Bottinelli et al. (1984) determined the distance to NGC 1156 as 3.9 Mpc ($(m-M)_0 = 27.98$ mag) by the B-band Tully-Fisher relation with a relatively large error ($\sim$ 1.2 mag) in the distance modulus (Karachentsev et al. 1996). Tully (1988) obtained a larger distance of 6.4 Mpc ($(m-M)_0 = 29.02 \pm 0.40$ mag) again from the Tully-Fisher relation and a heliocentric velocity of 372 km s^{-1}. Using the magnitudes of RSG and BSG candidates, Karachentsev et al. (1996) obtained the distance of $d = 7.8 \pm 0.5$ Mpc ($(m-M)_0 = 29.46 \pm 0.15$ mag) to NGC 1156, which is the mean value of $(m-M)_0 = 29.61$ mag (obtained from the three RSGs with a mean V-band magnitude of $\langle V(3R)\rangle = 22.45$ mag) and $(m-M)_0 = 29.32$ mag (obtained from the three BSGs with $\langle B(3B)\rangle = 21.31$ mag). They searched for RSG and BSG candidates only outside of the central crowded areas to avoid the crowding in the inner regions and obtained a mean apparent magnitude for the three brightest red stars of $\langle V(3R)\rangle = 22.45$ mag, and that for the three brightest blue stars of $\langle V(3B)\rangle = 21.24$ mag.

With non-variable absolute visual magnitudes up to $M_V \simeq -9.5$ mag, the brightest stars method is quite useful in estimating the distances to galaxies without the necessity of repeated observations (Hubble 1936; Humphreys 1987; Sandage & Carlson 1988; Karachentsev & Tikhonov 1994; Rozanski & Rowan-Robinson 1994; Lyo & Lee 1997; Kudritzki et al. 2003; Bresolin 2003; Vaduvescu et al. 2005; Kudritzki et al. 2008, 2010). Instead of the single brightest star, the average magnitude of the three brightest stars have been used to minimize the effects of misidentifying the brightest individual star and to reduce the stochastic effect in obtaining the mean luminosity of the brightest stars (Rozanski & Rowan-Robinson 1994; Lyo & Lee 1997). While Rozanski & Rowan-Robinson (1994) claimed rather larger errors in this method of 0.58 mag and 0.90 mag, respectively, for the brightest red and blue stars, Karachentsev & Tikhonov (1994) suggested much smaller errors of 0.30 mag and 0.45 mag for the brightest red and blue stars, respectively. Using new CCD-based data for 17 galaxies, Lyo & Lee (1997) showed that the uncertainties in the distance moduli determined by the brightest red and blue stars are 0.37 mag and 0.55 mag, respectively, concluding that the brightest RSGs might be useful in determining the distances to resolved late-type galaxies. They proposed new calibration equations :

$$\langle M_V(3)_{RSG}\rangle = 0.21M_B^T - 3.84,\ \sigma(M_V) = 0.37\,\mathrm{mag} \quad (2)$$

and

$$\langle M_B(3)_{BSG}\rangle = 0.30M_B^T - 3.02,\ \sigma(M_B) = 0.55\,\mathrm{mag}. \quad (3)$$

In order to make it free from any contamination by foreground stars and to select the three brightest blue and red stars, we consider stars bluer than $B-V = 0.4$ mag (in $(B, B-V)$ CMD) and redder than $B-V = 2.0$ mag (in $(V, B-V)$ CMD), respectively (Rozanski & Rowan-Robinson 1994). In figure 7, we show the selected supergiant stars: pentagons are the three brightest blue stars and the open circles are the three brightest red stars, while the triangles and squares in panels (c) and (d) are the brightest blue and red, respectively, stars selected in Karachentsev et al. (1996). Table 2 lists the equatorial coordinates and photometry results of the selected BSG and RSG stars. While we denote $V(3)$ as the average V-band magnitude of the three brightest stars selected in the V-band, it is worth noting here that the brightest RSG stars in $V(3)$ or $K(3)$ will not, in general, be the same stars as in $I(3)$ or $R(3)$, and this situation is the same for the brightest BSGs (Rozanski & Rowan-Robinson 1994). It is natural that similar but not the same stars are selected between our study and that of Karachentsev et al. (1996) considering the different areas of the studies: we use the *HST* images of the central $26'' \times 29''$ region of NGC 1156, while Karachentsev et al. (1996) searched for supergiant candidates only outside the central/crowded areas in their $80'' \times 120''$ CCD images. The mean magnitudes of the three brightest BSGs are $\langle B(3B)\rangle = 21.943$ mag and

$\langle V(3B)\rangle = 21.680$ mag and the mean color is $\langle(B-V)(3B)\rangle = 0.263$ mag, where 3B denotes the three brightest BSGs. The redder $(V-I)$ colors of the BSGs in this study ($\langle(V-I)\rangle = 0.392$ mag) over those of the BSGs in Karachentsev et al. (1996) ($\langle(V-I)\rangle = 0.077$ mag) might be due to the crowding of more dust and star forming regions in the central area of NGC 1156 that caused more reddening. The mean magnitudes of the three brightest RSGs in this study ($\langle V(3R)\rangle = 22.758$ mag, $\langle I(3R)\rangle = 20.871$ mag) are somewhat fainter than those of the RSGs in Karachentsev et al. (1996) ($\langle V\rangle = 22.443$ mag, $\langle I\rangle = 20.317$ mag) : $\langle V\rangle_{this\ study} - \langle V\rangle_{Karachentsev} = 0.315$ mag and $\langle I\rangle_{this\ study} - \langle I\rangle_{Karachentsev} = 0.554$ mag.

Using the total blue absolute magnitude of NGC 1156 ($M_B^T = -18.64$ mag) given by Barazza et al. (2001) (we reddened $M_{B,0}^T$ into M_B^T again using $A_B = 0.96$ mag as given in their study) and equation (2), we obtain the mean total visual absolute magnitude of $\langle M_V(3)_{RSG}\rangle = -7.75$ mag. Using the average V magnitude of the three brightest RSGs derived in the previous paragraph ($\langle V(3R)\rangle = 22.758$ mag), we get the distance modulus of $(m-M)_0 = 22.758 + 7.75 - 3.1E(B-V) = 29.423$ mag. Using this value, iteratively, to derive the total blue absolute magnitude of NGC 1156 assuming $B_T = 11.78$ mag (Barazza et al. 2001) and the total reddening of $A_B = 1.45$ mag (section 4.2), we get $M_B^T = -19.093$ mag. Inserting this value into the equation (2) and iterating this process until the values converge, we obtain $M_B^T = -19.22$ mag, $\langle M_V(3)_{RSG}\rangle = -7.88$ mag, and the distance modulus $(m-M)_0 = 29.55$ mag ($d = 8.1$ Mpc).

Similarly, using the total blue absolute magnitude of NGC 1156 ($M_B^T = -18.64$ mag) given by Barazza et al. (2001) and equation (3), we get the mean total blue absolute magnitude of $\langle M_B(3)_{BSG}\rangle = -8.61$ mag. Using the average B magnitude of the three brightest BSGs derived above ($\langle B(3B)\rangle = 21.943$ mag), we get the distance modulus of $(m-M)_0 = 21.943 + 8.61 - 4.14E(B-V) = 29.104$ mag. Using this value to derive again the total blue absolute magnitude of NGC 1156 and iterating the process until the values converge, we get $M_B^T = -18.83$ mag, $\langle M_B(3)_{BSG}\rangle = -8.67$ mag, and the distance modulus $(m-M)_0 = 29.16$ mag ($d = 6.8$ Mpc).

The average of the distance moduli obtained from using the BSGs and RSGs is $(m-M)_0 = 29.36 \pm 0.20$ mag ($d = 7.4 \pm 0.7$ Mpc). Since the uncertainties of the distance estimates from these two methods are different, we use different weights for each of them. The errors in the distance estimation methods using BSGs and RSGs, respectively, are 0.90 mag : 0.58 mag (1.55 : 1) in the study of Rozanski & Rowan-Robinson (1994), 0.45 mag : 0.30 mag (1.50 : 1) in that of Karachentsev & Tikhonov (1994), and 0.55 mag : 0.37 mag (1.49 : 1) in that of Lyo & Lee (1997). The mean values of the three estimates of the errors for the BSGs and RSGs are 0.63 mag and 0.42 mag, respectively, and the ratio is 1.50 : 1. Giving single weight to the distance estimate from the BSGs and a weight of 1.5 to that from the RSGs, we finally obtain $(m-M)_0 = 29.39 \pm 0.20$ mag ($d = 7.6 \pm 0.7$ Mpc). This result is in very good agreement with that derived by Karachentsev et al. (1996), while somewhat larger than that of Tully (1988). The fact that the distance estimate of this study is very similar to that of Karachentsev et al. (1996) could be considered reasonable because the magnitudes of the selected BSGs and RSGs are not much different and the studied areas of the two studies are located close to each other.

5. DISCUSSION

While de Vaucouleurs et al. (1991) lists the angular diameter of NGC 1156 to be $3.3'$, our study and that of Karachentsev et al. (1996) have used, respectively, only the HST data of the central $26'' \times 29''$ area and the SAO 6 m telescope data of the central $80'' \times 120''$ area. This means the present study covered only 2.5% of the area of NGC 1156 and that of Karachentsev et al. (1996) 31.2%. In fact, in order to select the true brightest stars in a galaxy, we would need to observe the entire area of the galaxy. It, therefore, might be easily speculated that there could be brighter stars in NGC 1156 than the brightest stars selected in the two studies above.

Figure 1 shows that the area covered by Karachentsev et al. (1996) includes most of the bar-like main body and most of the star forming regions of NGC 1156, and it seems there may not be many, if any, brighter stars outside of the area studied by Karachentsev et al. (1996). The fact

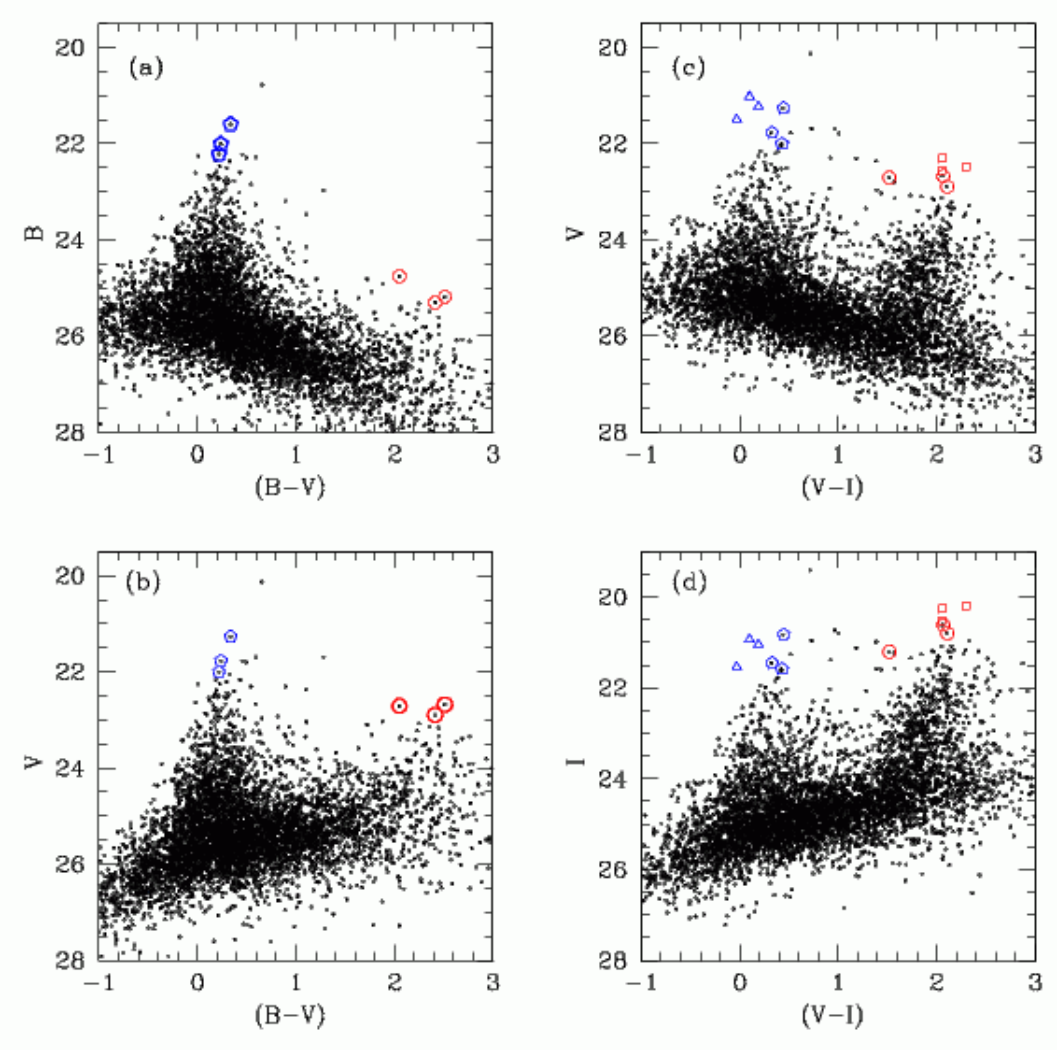

Fig. 7.— The location of the selected blue supergiants (BSGs) and red supergiants (RSGs) in (a) $(B, B-V)$ CMD, (b) $(V, B-V)$ CMD, (c) $(V, V-I)$ CMD, and (d) $(I, V-I)$ CMD. Pentagons and open circles are the BSG and RSG stars, respectively, selected in this study, while triangles and squares in panels (c) and (d) are the brightest blue and red, respectively, stars selected in Karachentsev et al. (1996). BSGs selected in the $(B, B-V)$ CMD (panel (a)) and RSGs selected in the $(V, B-V)$ CMD (panel (b)) are denoted boldly in each panel.

that our study have used a smaller area than that of Karachentsev et al. (1996) is consistent with somewhat fainter $\langle V \rangle$ magnitudes for both the BSGs ($\Delta V = V_{This\ study} - V_{Karachentsev} \sim 0.44$ mag) and the RSGs ($\Delta V \sim 0.32$ mag) selected in this study as shown in figure 7 (c). The $\langle I \rangle$ magnitude for the RSGs selected in this study is quite fainter than that of Karachentsev et al. (1996) ($\Delta I = I_{This\ study} - I_{Karachentsev} \sim 0.55$ mag), but the $\langle I \rangle$ magnitude for the BSGs selected in this study is only a little fainter than that of Karachentsev et al. (1996) ($\Delta I \sim 0.12$ mag; figure 7 (d)). Although the smaller area covered by the *HST* images in this study compared to that of Karachentsev et al. (1996) renders fainter mean magnitudes of the brightest stars, the new calibration for the brightest stars (from Lyo & Lee (1997)) and the new estimate of the total reddening to NGC 1156 used in this study give almost the same distance. It is still possible, though, that we might get brighter magnitudes for the brightest stars (and smaller distance modulus), if we observe a larger area than that of Karachentsev et al. (1996) ($r \gtrsim 0.9'$).

The study of Karachentsev et al. (1996) and our study have used different observation data and different regions to search for the brightest stars: the former focused only on the outer regions in their $80'' \times 120''$ images to avoid the central crowded areas and the latter used only the central $26'' \times 29''$ area of NGC 1156. Therefore, we can obtain more reliable results if we combine the data on the brightest stars from these two studies. The selection of three brightest RSGs among the six RSGs in the two studies give the same stars as in the study of Karachentsev et al. (1996) since all of their stars are brighter than those of the present study. Using the three RSGs of Karachentsev et al. (1996) with $\langle V(3R) \rangle = 22.45$ mag and the equation (2), we obtain the distance modulus of $(m-M)_0 = 29.16$ mag ($d = 6.8$ Mpc).

Karachentsev et al. (1996) used only V and I bands for their study. They used these two bands to search for both BSGs and RSGs and they obtained the mean B magnitude of the three BSGs ($\langle B(3B) \rangle = 21.31$ mag) from conversion of the mean V magnitude and $(V-I)$ color ($\langle V(3B) \rangle = 21.24$ mag, $\langle (V-I) \rangle = 0.08$ mag). Although the B magnitude of each of the three BSGs in the study of Karachentsev et al. (1996) is not known, we might be able to assume that they are all brighter than any of the BSGs used in the present study considering the larger magnitude difference in V (figure 7 (c)) than that in I (figure 7 (d)) : $\Delta V = \langle V_{This\ study} \rangle - \langle V_{Karachentsev} \rangle \sim 0.44$ mag and $\Delta I = \langle I_{This\ study} \rangle - \langle I_{Karachentsev} \rangle \sim 0.12$ mag. Using the three brightest BSGs of Karachentsev et al. (1996) among the six BSGs in the two studies and the equation (3), we get $\langle B(3B) \rangle = 21.31$ mag, which gives us the distance modulus of $(m-M)_0 = 28.26$ mag ($d = 4.5$ Mpc).

The weighted mean of the distance estimates from using BSGs and RSGs using weights of 1 and 1.5, respectively, is $(m-M)_0 = 28.80 \pm 0.20$ mag ($d = 5.8 \pm 0.5$ Mpc), while the unweighted mean is $(m-M)_0 = 28.71 \pm 0.50$ mag ($d = 5.5 \pm 1.4$ Mpc). Using the revised calibration of the BSGs and RSGs in Lyo & Lee (1997) and the newly obtained total reddening to NGC 1156 in this study, we derive a distance to this galaxy smaller than those obtained in section 4.3 and in Karachentsev et al. (1996). Future wide-field imaging of NGC 1156 at least in B and V-bands might be helpful in resolving this issue and determining more accurate distance to NGC 1156.

The mean magnitudes and color of the BSGs obtained in this study are $\langle V(3B) \rangle = 21.68$ mag, $\langle I(3B) \rangle = 21.29$ mag, and $\langle (V-I)(3B) \rangle = 0.39$ mag, and those of the RSGs obtained in this study are $\langle V(3R) \rangle = 22.76$ mag, $\langle I(3R) \rangle = 20.87$ mag, and $\langle (V-I)(3R) \rangle = 1.89$ mag. On the other hand, the mean magnitudes and color of the BSGs obtained by Karachentsev et al. (1996) are $\langle V(3B) \rangle = 21.24$ mag, $\langle I(3B) \rangle = 21.17$ mag, and $\langle (V-I)(3B) \rangle = 0.08$ mag, and those of the RSGs obtained by Karachentsev et al. (1996) are $\langle V(3R) \rangle = 22.44$ mag, $\langle I(3R) \rangle = 20.32$ mag, and $\langle (V-I)(3R) \rangle = 2.13$ mag. All the magnitudes obtained in our study are $0.12-0.55$ mag fainter than those of Karachentsev et al. (1996), while the situation is different for the $(V-I)$ color : the mean $(V-I)$ color for the BSGs obtained in our study is 0.32 mag redder than that of Karachentsev et al. (1996), while that for the RSGs is 0.24 mag bluer than that of Karachentsev et al. (1996). It could be possible that there occurs larger absorption in the central part of NGC 1156, which affects more for the BSGs than the RSGs. Nevertheless, since we accurately estimated the reddening value in the central part of the galaxy and applied it in deter-

mining the distance, the distance values obtained in this study are not affected much by the differences of reddening values in our study and in the study of Karachentsev et al. (1996).

All the studies performed in the 1990s, including those of Karachentsev & Tikhonov (1994), Rozanski & Rowan-Robinson (1994), and Lyo & Lee (1997), used the $(B-V)$ color to select both BSGs and RSGs. The wide use of CCDs since then have produced colors using longer wavelengths such as $(V-I)$ thanks to the good sensitivities of CCD detectors at these wavebands. It might be helpful if we could use this $(V-I)$ color in selecting or investigating the RSGs rather than the $(B-V)$ color. Using the $(V-I)$ colors for the RSGs assembled in Lyo & Lee (1997) together with those for NGC 1156 selected in this study, we plot the $(V, V-I)$ and $(I, V-I)$ CMDs in figure 8 to show the $(V-I)$ color distribution of the RSGs. While many RSGs are gathered near $(V-I) \sim 2$ mag, the whole color range of the RSGs is $1.5 mag \lesssim (V-I) \lesssim 3.5$ mag.

Figure 7 shows that among the three selected RSGs, RSG2 is bluest both in $(B-V)$ and $(V-I)$ colors. The $(V-I)$ color of this star ($(V-I) = 1.51$ mag) is almost at the blue edge in the color range shown in figure 8. If we ignore this star and select again three RSGs in figure 7(c), the somewhat fainter and redder star with $V = 22.8$ mag and $(V-I) = 1.56$ mag will be chosen, and this does not much affect the resultant distance estimate to NGC 1156.

6. SUMMARY

Using the $UBVI$ archive HST ACS/HRC images of the dIrr galaxy NGC 1156, we performed DOLPHOT photometry, constructed various combinations of CMDs, and estimated the total (foreground + internal) reddening and distance to this galaxy. Although the CMDs are not deep enough to detect the TRGB due to the short exposure times of the HST images, they are good enough to draw a $(U-B, B-V)$ color-color diagram to determine the total interstellar reddening of $E(B-V) = 0.35 \pm 0.05$ mag and to select the three BSGs and three RSGs, which allowed us to determine the distance to this galaxy, $d = 7.6 \pm 0.7$ Mpc ($(m-M)_0 = 29.39 \pm 0.20$ mag).

The CMDs obtained in this study are quite similar to those of NGC 6822 (Gallart et al. 1996) (figure 15, $(V, B-V)$ CMD and figure 17, $(I, V-I)$ CMD), NGC 3109 (Minniti et al. 1999) (figure 2, $(I, V-I)$ and $(V, V-I)$ CMDs), WLM (Minniti & Zijlstra 1997) (figure 5, $(V, V-I)$ and $(I, V-I)$ CMDs), and/or IC 1613 (Freedman 1988) (figure 4, $(V, B-V)$ CMD and figure 5, $(I, V-I)$ CMD). Since NGC 1156 is located much farther than these late-type dwarf galaxies, it is necessary to get deeper imaging of NGC 1156 to obtain deep enough photometry so that we can estimate the distance more reliably using the TRGB method or perform a detailed study of the stellar populations of this galaxy.

The authors are thankful to the anonymous referee for useful comments that improved the manuscript. H.S.P. was supported by Mid-career Researcher Program through NRF grant funded by the MEST (No.2010-0013875). S.C.K., J.K., J.H.L., and C.H.R. are members of the Dedicated Researchers for Extragalactic AstronoMy (DREAM) team in the Korea Astronomy and Space Science Institute (KASI). This paper is based on observations made with in the NASA/ESA Hubble Space Telescope, obtained from the data archive at the Space Telescope Science Institute, which is operated by AURA, Inc., for NASA under contract NAS 5-26555. This research has made use of NASA's Astrophysics Data System Abstract Service and the NASA/IPAC Extragalactic Database (NED), which is operated by the Jet Propulsion Laboratory, California Institute of Technology, under contract with the National Aeronautics and Space Administration.

REFERENCES

Barazza, F. D., Binggeli, B., & Prugniel, P. 2001, A&A, 373, 12

Bertelli, G., Bressan, A., Chiosi, C., Fagotto, F., & Nasi, E. 1994, A&AS, 106, 275

Bono, G., Caputo, F., Marconi, M., & Musella. I. 2010, ApJ, 715, 277

Bottinelli, L., Gouguenheim, L., Paturel, G., & de Vaucouleurs, G. 1984, A&AS, 56, 381

Bresolin, F. 2003, Stellar Candles for the Extra-

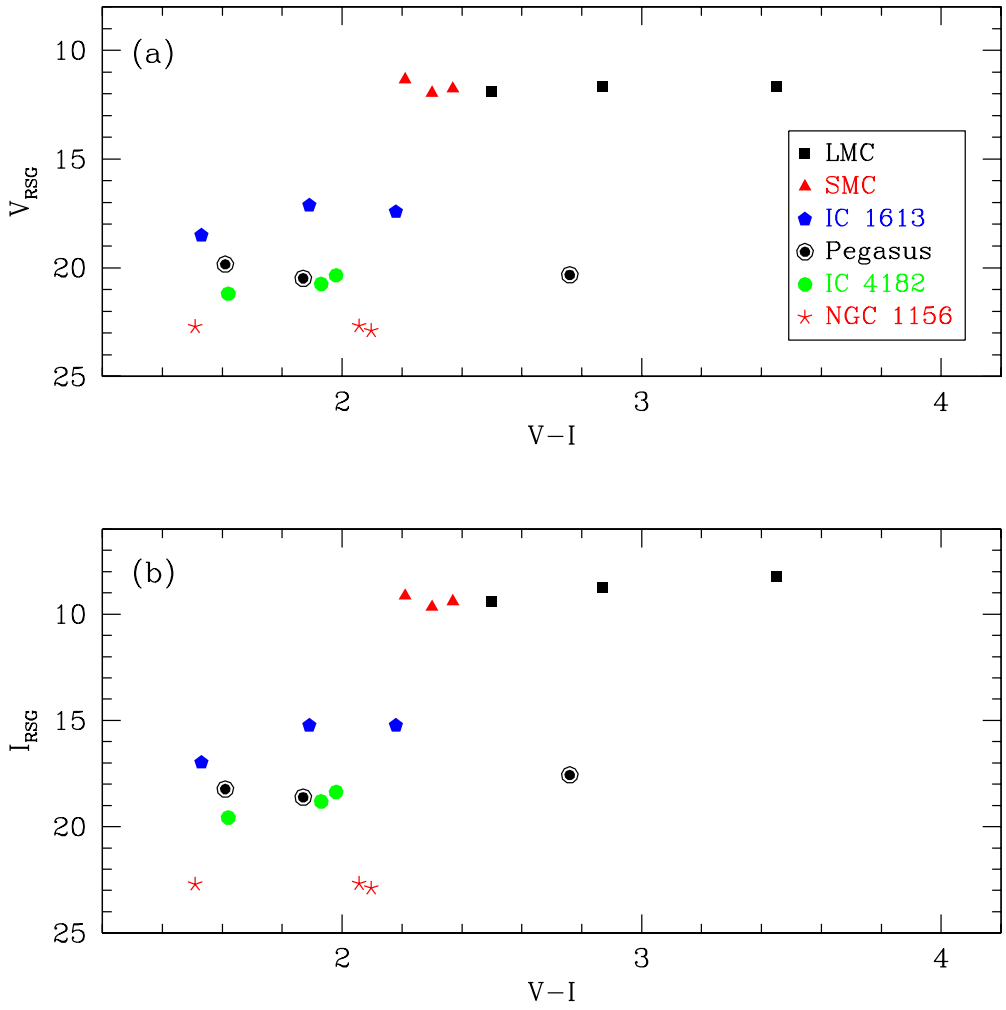

Fig. 8.— The (a) $(V, V-I)$ and (b) $(I, V-I)$ CMDs showing the RSGs assembled and used in Lyo & Lee (1997) and those selected in this study for NGC 1156. The symbols for the six galaxies including NGC 1156 are shown in box in panel (a).

galactic Distance Scale, Edited by D. Alloin and W. Gieren, Lecture Notes in Physics, 635, 149

Broeils, A. H., & van Woerden, H. 1994, A&AS, 107, 129

Burstein, D., & Heiles, C. 1984, ApJS, 54, 33

Cardelli, J. A., Clayton, G. C., & Mathis, J. S. 1989, ApJ, 345, 245

Cioni, M. -R. L., & Habing, H. J. 2005, A&A, 429, 837

Cole, A. A., et al. 2007, ApJ, 659, L17

Dale, D. A., et al. 2000, AJ, 120, 583

de Vaucouleurs, G., de Vaucouleurs, A., Corwin, H. G., Jr., Buta, R. J., Paturel, G., & Fouqué, P. 1991, Third Reference Catalogue of Bright Galaxies (Springer, New York)

Dolphin, A. E. 2000a, PASP, 112, 1383

Dolphin, A. E. 2000b, PASP, 112, 1397

Freedman, W. L. 1988, AJ, 96, 1248

Gallart, C., Aparicio, A., & Vilchez, J. M. 1996, AJ, 112, 1928

Gunn, J. E., & Stryker, L. L. 1983, ApJS, 52, 121

Haynes, M. P., van Zee, L., Hogg, D. E., Roberts, M. S., & Maddalena, R. J. 1998, AJ, 115, 62

Hubble, E. P. 1936, ApJ, 84, 158

Humphreys, R. M. 1987, PASP, 99, 5

Hunter, D. A., Rubin, V. C., Swaters, R. A., Sparke, L. S., & Levine, S. E. 2002, ApJ, 580, 194

Hunter, D. A., & Elmegreen, B. G. 2004, AJ, 128, 2170

Isobe, T., Feigelson, E. D., Akritas, M. G., & Babu, G. J. 1990, ApJ, 364, 104

James, P. A., et al. 2004, A&A, 414, 23

Karachentsev, I., & Tikhonov, N. A. 1994, A&A, 286, 718

Karachentsev, I., Musella, I., & Grimaldi, A. 1996, A&A, 310, 722

Kim, S. C., & Lee, M. G. 1998, J. Korean Astron. Soc., 31, 51

Kudritzki, R. P., Bresolin, F., & Przybilla, N. 2003 ApJ, 582, L83

Kudritzki, R. P., Urbaneja, M. A., Bresolin, F., & Przybilla, N. 2008, Physica Scripta, 133, 14039

Kudritzki, R.-P. 2010, AN, 331, 459

Kyeong, J., Sung, E.-C., Kim, S. C., Sohn, S. T., & Sung, H.-I. 2006, J. Korean Astron. Soc., 39, 89

Kyeong, J., Sung, E.-C., Kim, S. C., & Chaboyer, B. 2010, J. Korean Astron. Soc., 43, 1

Lee, M. G., Freedman, W. L., & Madore, B. F. 1993, ApJ, 417, 553

Lyo, A.-R., & Lee, M. G. 1997 J. Korean Astron. Soc., 30, 27

Marigo, P., Girardi, L., Bressan, A., Groenewegen, M. A. T., Silva, L., & Granato, G. L. 2008, A&A, 482, 883

Minchin, R. F., et al. 2010, AJ, 140, 1093

Minniti, D., & Zijlstra, A. A. 1997, AJ, 114, 147

Minniti, D., Zijlstra, A. A., & Alonso, M. V. 1999, AJ, 117, 881

Rozanski, R., & Rowan-Robinson, M. 1994, MNRAS, 271, 530

Saha, A., Shaw, R. A., Claver, J. A., & Dolphin, A. E. 2011, PASP, 123, 481

Sandage, A., & Binggeli, B. 1984, AJ, 89, 919

Sandage, A., & Carlson, G. 1988, AJ, 96, 1599

Saviane, I., Ivanov, V. D., Held, E. V., Alloin, D., Rich, R. M., Bresolin, F., & Rizzi, L. 2008, A&A, 487, 901

Schlegel, D. J., Finkbeiner, D. P., & Davis, M. 1998, ApJ, 500, 525

Sirianni, M. et al. 2005, PASP, 117, 1049

Swaters, R. A., van Albada, T. S., van der Hulst, J. M., & Sancisi, R. 2002, A&A, 390, 829

Tully, R. B. 1988, Nearby Galaxies Catalog, (Cambridge University Press, Cambridge), 22

Vaduvescu, O., McCall, M. L., Richer, M. G., & Fingerhut, R. L. 2005, AJ, 130, 1593

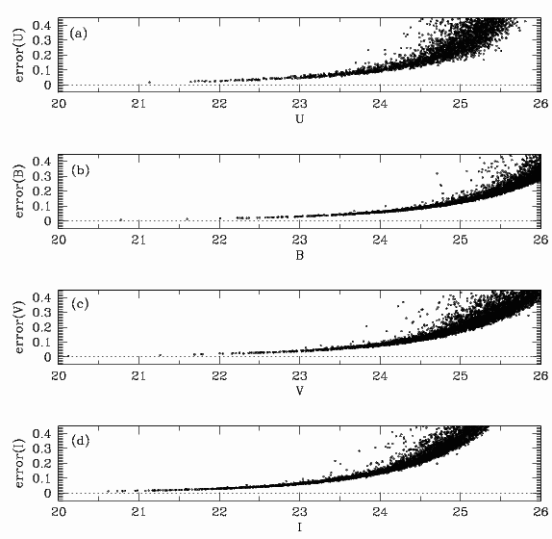

Fig. 3.— Photometric errors from the DOLPHOT package as a function of magnitude. Only stars with DOLPHOT object type 1 (good star; $N = 5580$) are plotted.

This 2-column preprint was prepared with the AAS LaTeX macros v5.2.

Table 1. Basic Information of NGC 1156

Parameter	Information	Reference
$\alpha_{J2000.0}$, $\delta_{J2000.0}$	$02^h\ 59^m\ 42.19^s$, $+25^\circ\ 14'\ 14.2''$	NASA/IPAC Extragalactic Database (NED)
l, b	$156.^\circ31$, $-29.^\circ20$	NED
Morphological type	IB(s)m V-VI	de Vaucouleurs et al. (1991)
Position angle (N through E)	39°	Hunter et al. (2002)
Angular diameter, D_0	$3.3'$	de Vaucouleurs et al. (1991)
Axial ratio	7.4	de Vaucouleurs et al. (1991)
Kinematical axes of the ionized gas, neutral gas, and stellar disks	84°	Hunter et al. (2002)
Inclination, i	42°	Bottinelli et al. (1984)
Radial velocity, v_r	375 ± 1 km s^{-1}	NED
Redshift, z	0.001251	NED
Distance modulus, $(m-M)_0$	29.02 ± 0.40 mag ($d = 6.4 \pm 1.2$ Mpc)	Tully (1988)
	29.46 ± 0.15 mag ($d = 7.8 \pm 0.5$ Mpc)	Karachentsev et al. (1996)
	29.39 ± 0.20 mag ($d = 7.6 \pm 0.7$ Mpc)	This study
Reddening, $E(B-V)$	0.35 ± 0.05 mag	This study
B_0, $M_{B,0}$	11.78 ± 0.10 mag[a], -17.68 mag[b]	Barazza et al. (2001)
B_0	11.56 mag[c]	Tully (1988)
B_0	11.61 mag[a]	Bottinelli et al. (1984)
B_0, $M_{B,0}$	12.32 mag, -17.85 mag[b,d]	de Vaucouleurs et al. (1991)
V_0	11.31 mag[a]	Barazza et al. (2001)
M_V	-18.67 mag[b]	Hunter & Elmegreen (2004)
R_0	10.91 mag[a]	Barazza et al. (2001)
R	11.91 ± 0.04 mag	James et al. (2004)
$(B-V)_0$	0.47[a]	Barazza et al. (2001)
$(B-R)_0$	0.87[a]	Barazza et al. (2001)
Effective radius, $r_{\rm eff}^B$, $r_{\rm eff}^V$, $r_{\rm eff}^R$	$31.58'', 34.28'', 35.48''$	Barazza et al. (2001)
Effective surface brightness, $\langle\mu\rangle_{\rm eff}^B$, $\langle\mu\rangle_{\rm eff}^V$, $\langle\mu\rangle_{\rm eff}^R$	21.28, 20.98, 20.66 mag arcsec^{-2}	Barazza et al. (2001)
flux density at $12, 25, 60, 100\mu$m	0.17, 0.55, 5.24, 10.48 Jy	Dale et al. (2000)
flux density at $6.75, 15\mu$m	0.09 ± 0.02, 0.14 ± 0.03 Jy	Dale et al. (2000)
H I flux	71.3 Jy km s^{-1}	Swaters et al. (2002)
	72.72 Jy km s^{-1}	Haynes et al. (1998)
	75.6 ± 6.4 Jy km s^{-1}	Minchin et al. (2010)
H I mass, M_{H_I}	$1.02 \times 10^9\ M_\odot$	Swaters et al. (2002)
	$(1.08 \pm 0.09) \times 10^9\ M_\odot$	Minchin et al. (2010)
H I line width[e], W_{50}	73 ± 3 km s^{-1}	Broeils & van Woerden (1994)
M_{H_I}/L_B	$0.56\ M_\odot/L_\odot$	Swaters et al. (2002)
Star formation rate, SFR	$0.71 \pm 0.07\ M_\odot$/yr	James et al. (2004)

[a] Only the foreground extinction is corrected
[b] Assuming d $= 7.8 \pm 0.5$ Mpc
[c] Both foreground and internal extinctions are corrected
[d] Assuming $A_B = 0.71$ mag
[e] Profile width at a level of 50% of the peak value, corrected for instrumental broadening

Table 2. Selected Blue and Red Supergiant Stars in NGC 1156[a]

ID	R.A.(J2000.0)[b]	Decl.(J2000.0)[c]	U	$Uerr$	B	$Berr$	V	$Verr$	I	$Ierr$
BSG1	2:59:41.96	25:14:33.6	21.130	0.017	21.598	0.013	21.263	0.014	20.827	0.015
BSG2	2:59:42.02	25:14:08.3	21.786	0.026	22.009	0.017	21.772	0.019	21.453	0.022
BSG3	2:59:41.48	25:14:13.8	21.834	0.028	22.221	0.022	22.004	0.025	21.584	0.028
RSG1	2:59:42.38	25:14:33.7	26.942	3.690	25.184	0.181	22.674	0.030	20.617	0.013
RSG2	2:59:42.12	25:14:27.9	25.513	0.607	24.757	0.110	22.708	0.031	21.199	0.019
RSG3	2:59:42.57	25:14:34.3	25.554	0.788	25.305	0.177	22.893	0.036	20.796	0.014

[a] BSGs are in the order of B-magnitudes and RSGs are in the order of V-magnitudes.
[b] in hours, minutes, and seconds
[c] in degrees, arcminutes, and arcseconds